A Dual Electrochrome of Poly-(3,4-Ethylenedioxythiophene) Doped by *N,N′*-Bis(3-sulfonatopropyl)-4-4′-bipyridinium—Redox Chemistry and Electrochromism in Flexible Devices

Shweta Bhandari,[a] Melepurath Deepa,*[a] Suman Pahal,[a] Amish G. Joshi,[a] Avanish Kumar Srivastava,[a] and Rama Kant[b]

An electrochromic zwitterionic viologen, *N,N′*-bis(3-sulfonatopropyl)-4-4′-bipyridinium, has been used for the first time for doping poly (3,4-ethylenedioxythiopene) (PEDOT) films during electropolymerization. Slow and fast diffusional rates for the monomer at deposition potentials of +1.2 and +1.8 V, respectively yielded the viologen-doped PEDOT films with granular morphology and with dendrite-like shapes. The dual electrochrome formed at +1.8 V, showed enhanced coloration efficiency, larger electrochemical charge storage capacity, and superior redox activity in comparison to its analogue grown at +1.2 V, thus demonstrating the role of dendritic shapes in amplifying electrochromism. Flexible electrochromic devices fabricated with the viologen-doped PEDOT film grown at +1.8 V and Prussian blue with an ionic liquid-based gel electrolyte film showed reversible coloration between pale and dark purple with maximum coloration efficiency of 187 $cm^2 C^{-1}$ at $\lambda = 693$ nm. The diffusional impedance parameters and switching kinetics of the device showed the suitability of this dual electrochrome formed as a single layer for practical electrochromic cells.

Introduction

For decades, there has been an enormous research interest in economically viable materials capable of modulating reflection or transmission through multiple hues. Electrochromic materials are best suited for different applications, such as high contrast displays, antiglare rearview mirrors, and energy-saving smart windows, owing to their ability to dynamically modulate incoming radiation through low power inputs.[1,2] Conducting polymers are attractive electrochromes by virtue of their high-contrast ratios, fast switching speeds, ease of color tuning, and high redox stability.[3] Amongst electrochromic polymers, poly-(3,4-ethylenedioxythiophene) (PEDOT) and its derivatives have always been forerunners because of their ease of processing, ease of switching between two redox states, and high chemical stability provided by an electron-donating ethylenedioxy group.[4–6] However, in terms of performance, there always remains a scope for further improvement to enhance electrochromic contrast and stability of materials and electrolytes for device applications.

For contrast improvement, derivatization of the monomer EDOT has already been accomplished by many researchers.[7–9] Ko et al.[10] associated an electrochromic viologen with EDOT; however, the route of derivatizing the monomer and its further polymerization are rather complicated processes. Similarly, post-polymerization functionalization of PEDOT has also been done[11] but there is a paucity of reports wherein electrochromic efficiency of such derivatized polymers has been studied. In yet another report, Stepp et al.[12] constructed electrochromic polyelectrolyte multilayers from a polyviologen and poly-(styrenesulfonate) by using alternating polyion solutions. Deep Longchamp et al.[13] also reported an increased electrochromic contrast by fabricating a layer by layer assembly of a PEDOT-polyviologen coating. However, in this method too, repeated coatings were cumbersome to carry out and charge trapping effects within the layers tended to influence the device operation.[10] Earlier, polypyrroles have been doped with electrochromic molecules, such as indigo carmine,[14] phthalocyanines,[15,16] and porphyrins.[17] Song et al.[18] studied electrochromism in detail for polypyrrole by incorporating 2,2′-azinobis (3-ethylbenzothiazoline-6-sulfonate) as a dopant which itself is electrochromic. However, to the best of our knowledge, no protocol involving the incorporation of an electrochromic zwitterionic viologen, as the charge compensating ion during electropolymerization of EDOT, has been reported to date. The usual viologen salts could not be used for fulfilling this objective as the bipyridinium moiety is positively charged and therefore, upon electropolymerization, only the negatively charged anion will associate with the polymer chain. Only in the case of a zwitterionic viologen, similar to the one used herein, the bipyridinium

[a] *S. Bhandari, Dr. M. Deepa, S. Pahal, Dr. A. G. Joshi, Dr. A. K. Srivastava*
National Physical Laboratory,
Dr. K. S. Krishnan road, New Delhi-110012 (India)
Fax: (+91)-11-45609310
E-mail: m_deepa@mail.nplindia.ernet.in

[b] *Dr. R. Kant*
Department of Chemistry,
University of Delhi, New Delhi - 110007 (India)

ion is covalently attached to the negatively charged propane sultone, and therefore the viologen (as a whole) will be incorporated as the dopant in PEDOT. Hence, in order to achieve the above target, we adopted a simple method wherein a salt of an organic viologen *N*,*N*′-bis(3-sulfonatopropyl)-4-4′-bipyridinium served as a dopant during polymerization of EDOT and also acted as a cathodic electrochrome.

We deposited films at two different constant potentials of +1.2 and +1.8 V in order to study the effect of applied potential on PEDOT nanostructures and compared the optical and redox properties of the resulting films. The films deposited at +1.2 and +1.8 V are referred to as PEDOT-Vio (1.2) and PEDOT-Vio (1.8), respectively. The motivation for growing films at high potentials stemmed from previous work by Lee et al.[19–21] in which nanotubular PEDOT was formed at high oxidation potentials. In addition, flexible electrochromic devices were also fabricated by employing viologen-doped PEDOT and Prussian blue (PB) deposited over conducting plastic substrates, as the coloring layers and an ionic liquid (IL)-based gel film as the electrolyte. Device performance evaluation demonstrated the applicability of these films to smart windows.

Results and Discussion

Deposition profiles

Current–time transients for the electrodeposition of the PEDOT films by subjecting the electrode from 0 V at t = 0, to +1.2 V and +1.8 V for the same duration of 120 s are shown in Figure 1. The double layer capacitance charge[22,23] causes the abrupt rise in the initial current under both potentials, and peak heights are 0.0080 and 0.0004 A under +1.8 and +1.2 V, respectively. An exponential decay follows (inset of Figure 1 a). This decay is gradual in the film deposited at +1.2 V and contrasts from the current response of the film deposited under +1.8 V in which the current decay is rapid. The subsequent increment in the current after decay, to acquire plateau behavior, is attributed to the diffusion limited oxidation of the monomer and it is rather small in the film deposited at +1.2 V, which is indicative of a slower diffusion rate. As the monomer diffuses slowly, due to a slow reaction rate (a function of an applied potential), the deposition occurs uniformly on the whole surface at +1.2 V[19] manifesting in a regular granular morphology. Contrary to this response, at +1.8 V, the diffusion of the monomer and the polymerization reaction are very fast (driven by the high potential), as a result of which the diffused monomer does not have sufficient time to deposit uniformly and therefore it is consumed immediately to form elongated fibers from different single nucleation sites. The SEM micrographs of the two films: PEDOT-Vio (1.2) and PEDOT-Vio (1.8), reflect the conclusions drawn on the basis of this hypothesis.

Further support is obtained from the apparent diffusion coefficient (*D*) for the monomeric species, determined using the Cottrell equation [Equation (1)]:[24]

$$I = nFAC_j\ (D_j)^{1/2}/(\pi)^{-1/2}(t)^{1/2} \qquad (1)$$

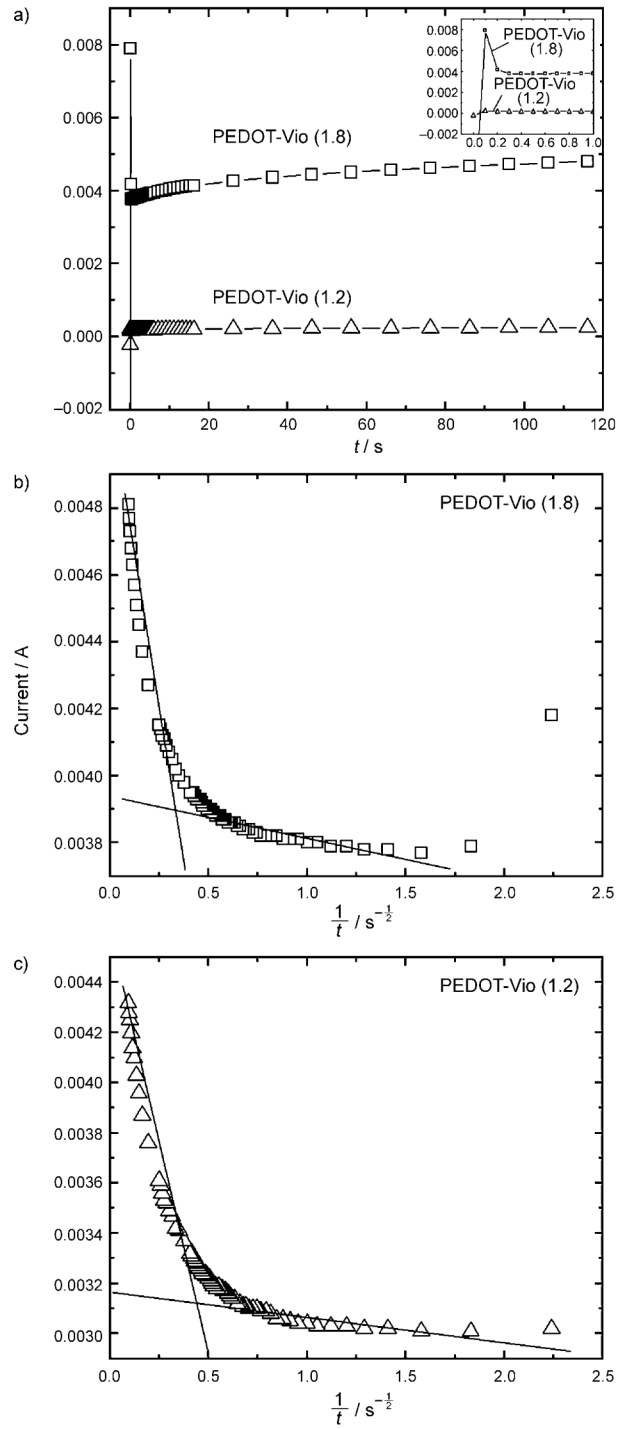

Figure 1. a) Current–time transients for oxidative electropolymerization of 3,4-(ethylenedioxythiophene) (0.1 M) in a Tween 20 (0.1 M) and *N*,*N*′-bis(3-sulfonatopropyl)-4-4′-bipyridinium (0.1 M) solution at two different constant potentials of +1.8 and +1.2 V for 120 s to yield PEDOT (1.8) (□) and PEDOT (1.2) (△) films, respectively, and b, c) their corresponding *I* versus $t^{-1/2}$ plots. Inset of (a) shows the deposition profiles in the early stages.

where *I* is the current in amperes, *n* is the number of electrons, *F* is the Faraday constant, C_j is the initial concentration in mol cm^{-3}, *t* is the time in seconds, and *A* is the area in cm^2.

From the slopes of current versus $t^{-1/2}$ plots, D was found to be 9.3×10^{-13} cm^{2}s^{-1} in 0.3–6.0 s and 3.4×10^{-10} cm^{2}s^{-1} in the 7.0–117.0 s range for PEDOT-Vio (1.8) (Figure 1b). Similarly, for the PEDOT-Vio (1.2) (Figure 1c), apparent D values were 1.6×10^{-13} cm^{2}s^{-1} in 0.2–2.3 s and 9.5×10^{-11} cm^{2}s^{-1} in 2.5-124.2 s. It is evident that in both time zones, during film deposition, the apparent D value is larger for PEDOT-Vio (1.8), thus experimentally proving that monomer to polymer transformation and deposition is faster in PEDOT-Vio (1.8).

Scanning electron microscopy (SEM) and transmission electron microscopy (TEM) studies

The SEM image of the PEDOT-Vio (1.2) (Figure 2a) is characterized by typical globular agglomerates usually found in surfactant-assisted polymerized films.[25–27] In contrast, the SEM images (Figure 2b and c) of PEDOT-Vio (1.8) reveals dendrite-like shapes (the individual strands are few microns in diameter) that are distributed randomly on the surface of the film deposited at +1.8 V (Figure 2b). Each individual dendrite (Figure 2c), has a common point of origin from where the elongated fibers spread out in all directions. The slow diffusion of the monomer and slow polymerization rate allow polymer deposition to occur uniformly without any preference at +1.2 V; whereas at +1.8 V, the process is so fast that the monomer molecules are immediately consumed for extending the polymer chain, which leads to the formation of the dendrite-like shapes. Figure 3 shows the formation of the different morphologies at the two potentials.

The bright field TEM image of the PEDOT-Vio (1.2) (Figure 4a) shows the featureless morphology of the film. Fine nanocrystallites trapped in an amorphous matrix are clearly visible in the corresponding high magnification image (Figure 4b). The crystalline component of the film is evident from the bright spotty rings in the selected area electron diffraction pattern (SADP) (inset of Figure 4b). The microstructure of PEDOT-Vio (1.8) contains similar attributes (Figure 4c); however, the level of crystallinity is much higher in this film which can be judged in absolute terms on the basis of the greater number of regions with lattice fringes prevalent in the film (Figure 4d). The bright spots superimposed over the diffuse rings confirm the crystalline component in the PEDOT-Vio (1.8) film (inset of Figure 4d). The interplanar spacings deduced from the HRTEM images were 9.7, 4.6, 3.0, and 2.3 Å for the PEDOT-Vio (1.2) film and 1.7 and 3.6 Å for the PEDOT-Vio (1.8) film. A chain stacking distance of 3.4 Å has been reported previously for PEDOT doped by tosylate ions,[28] which is rather close to $d = 3.6$ Å for the PEDOT-Vio (1.8) film. This short interchain distance of 3.4 Å was previously shown to increase conductivity by the virtue of orbital overlap, in the case of PEDOT-tosylate.[28] A similar line of reasoning accounts for the higher dc conductivity observed for the as-fabricated PEDOT-Vio (1.8) (2.6 mS cm^{-1}) in comparison to 1.1 mS cm^{-1} for the PEDOT-Vio (1.2) film. These dc conductivities were obtained from the quasi-ohmic (straight line) I–V plots recorded for the films in a configuration described earlier in more detail.[29]

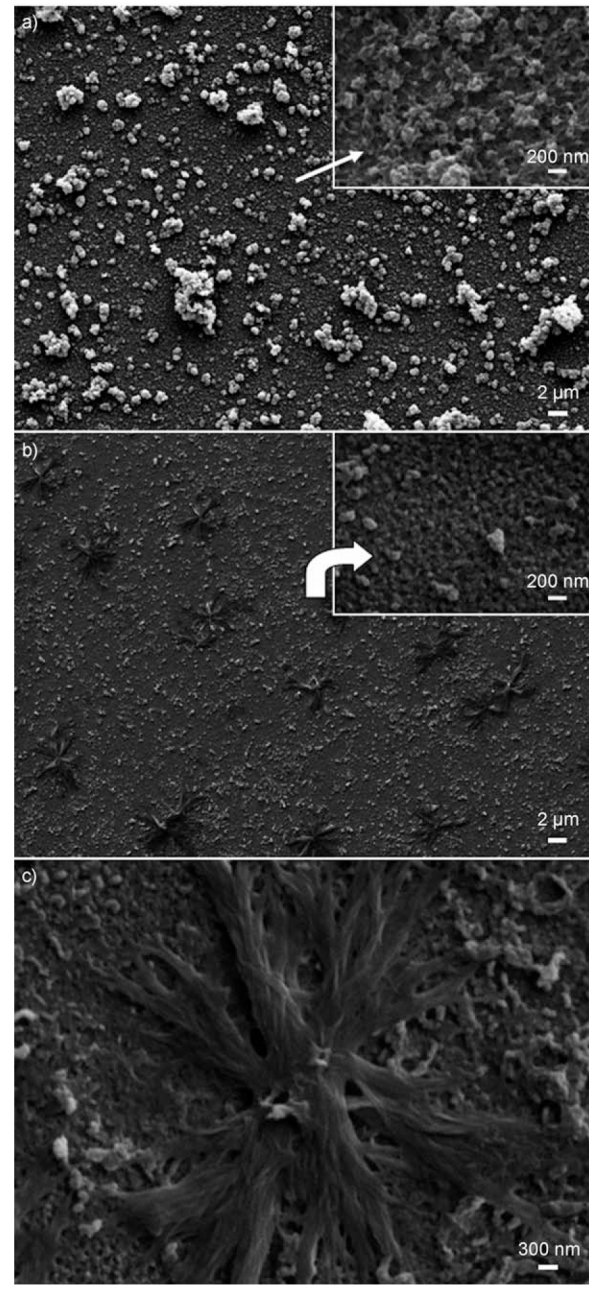

Figure 2. SEM images of a) PEDOT-Vio (1.2) film showing the globular surface morphology, b) and c) PEDOT-Vio (1.8) film, where (b) shows the random distribution of dendrite like shapes on the surface and (c) gives an enlarged view of a dendritic shape. Insets of (a) and (b) are the corresponding high magnification images at 25 000× and 20 000×, respectively.

FTIR and X-ray photoelectron spectroscopy (XPS) studies

The FTIR reflectance spectra of the two films: PEDOT-Vio (1.8) and PEDOT-Vio (1.2) are shown in Figure 5. The difference in deposition potentials results in different resonant conformations of the PEDOT chains in the two films which are clearly observable in the spectral profiles of the two. The band at 1430 cm^{-1}, corresponding to the symmetric C_α–C_β (–O) stretching mode is observed only in the spectrum of the PEDOT film grown at +1.8 V.[30] This peak is not seen in the spectrum of

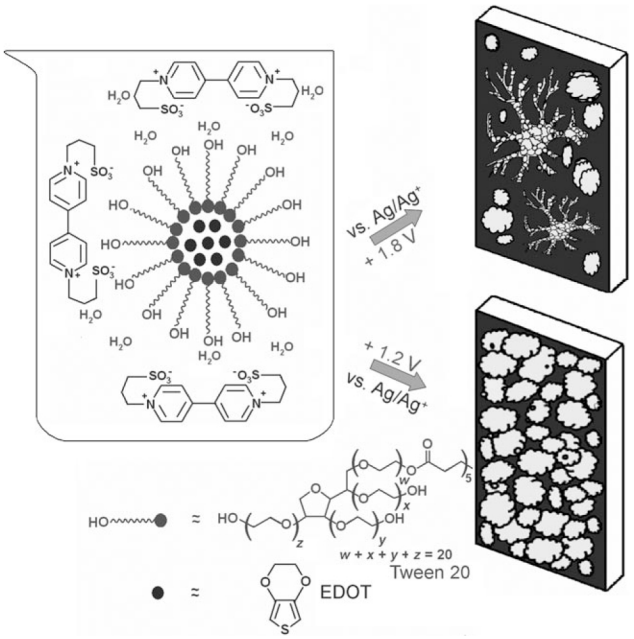

Figure 3. The formation of the PEDOT-Vio (1.8) and PEDOT-Vio (1.2) films with distinctly different morphologies from the solution containing EDOT, Tween 20, and *N*,*N*′-bis(3-sulfonatopropyl)-4-4′-bipyridinium at two dc potentials of +1.8 and +1.2 V, respectively.

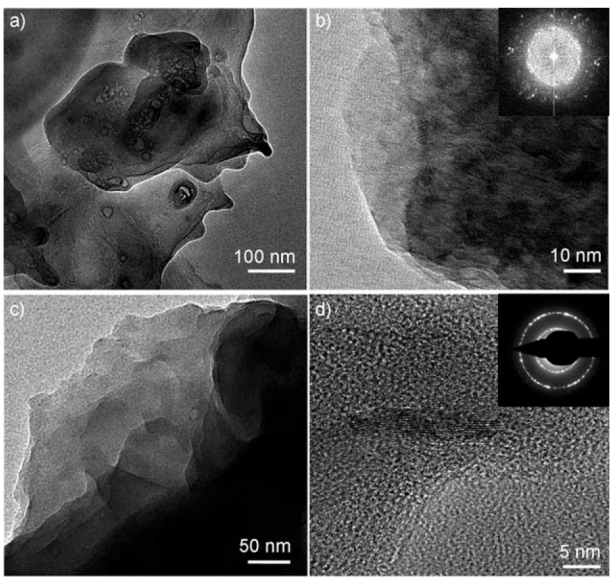

Figure 4. HRTEM images of a, b) PEDOT-Vio (1.2) and c, d) PEDOT-Vio (1.8) films and corresponding SADPs with spotty halo rings in insets of (b) and (d).

the film deposited at +1.2 V. Instead, an absorption at 1465 cm^{-1} is observed, which is characteristic of the symmetric C_α=C_β (-H) stretch vibration, thus illustrating the prominence of the benzoid states in this film. Greater delocalization of the conjugated π-electrons over the PEDOT chain in the expanded coil conformation, as compared to compact coiled one, results in higher charge mobility. A correlation of the quinoid with expanded coil conformation and that of the benzoid form with the compact coiled form has been reported.[31,32] The C_β–C_β stretching vibration[30] at 1362 cm^{-1} is only present in the film deposited at +1.8 V. Furthermore, the C_α–$C_{\alpha'}$ inter-ring stretch frequency upshifts from 1247 to 1255 cm^{-1}, ongoing from the deposition potential of +1.2 to +1.8 V, which suggests the formation of C_α=$C_{\alpha'}$ in PEDOT-Vio (1.8). Neither the film deposited at +1.2 V nor the one grown at +1.8 V show any peak due to the ν(C=O) mode, thereby providing clear evidence for the fact that both the films are not overoxidized. Deposition at high potentials, therefore, is not necessarily accompanied by over oxidation or ring-scission.

The incorporation of the viologen dopant, *N*,*N*′-bis(3-sulfonatopropyl)-4-4′-bipyridinium in PEDOT-Vio (1.8), is further confirmed from the elemental composition deduced from the XPS core level spectra of C, O, S, and N (Figure 6). For PEDOT-Vio (1.8), the C(1s) photoemission, after fixing the full width at half maximum (FWHM) at 2.2 eV, has been deconvoluted into multiple components with peaks at 284.1, 285.0, 285.7, and 287.6 eV (Figure 6a). The first two lower energy peaks arise from the C–C and C–S linkages in PEDOT and the viologen dopant. Since these bonds exist in both the polymer backbone and the dopant ion, it is difficult to identify the independent contributions of the dopant and polymer from the C(1s) spectrum. The carbon component at 285.7 eV is due to C–N, suggesting viologen inclusion and the peak of the highest binding energy is due to C–O in PEDOT. The I_{C-N} contribution was 18%. The O(1s) signal (FWHM = 2.43 eV) is constituted of two components (Figure 6b): the lower energy one with a higher intensity centered at 530.4 eV corresponds to S=O of the dopant (contribution is 61%), and the second peak at 531.9 eV is ascribed to the oxygen of the C–O–C bonds in the polymer chain.

Sulfur, which is omnipresent in both the polymer backbone and the dopant, produces the spin–spin doublet S($2p_{1/2}$) and S($2p_{3/2}$) with a energy split of 1.2 eV and a relative intensity of 1:2 (Figure 6c).[33,34] Peaks at lower binding energies of 158.2 and 159.4 eV correspond to spin–spin doublets of the sulfur atoms in PEDOT whereas the higher binding energy peaks at 160.2 and 161.4 eV correspond to the sulfur atoms of the viologen dopant. The core level spectrum of N(1s) (Figure 6d) indubitably affirms that the viologen dopant is incorporated in the polymer chain. The deconvolution of the broad envelope yielded independent contributions from the –N= and the positively charged N^+ species of the viologen at 399.8 and 401.1 eV, respectively. This result is in accordance with the assignments made for a nitrogen-containing compound formed as a result of a reaction between vinyl benzyl chloride-graft copolymerized films with 4-4′-bipyridine and benzyl chloride.[35] Here, the level of doping in the PEDOT-Vio (1.8) film by *N*,*N*′-bis(3-sulfonatopropyl)-4-4′-bipyridinium as deduced from the $I_{N(viologen)}/I_{C(total)}$ atomic ratio was 0.28, using areas under nitrogen and carbon peaks after applying a baseline correction from the survey spectrum (see the Supporting Information, Figure S1).

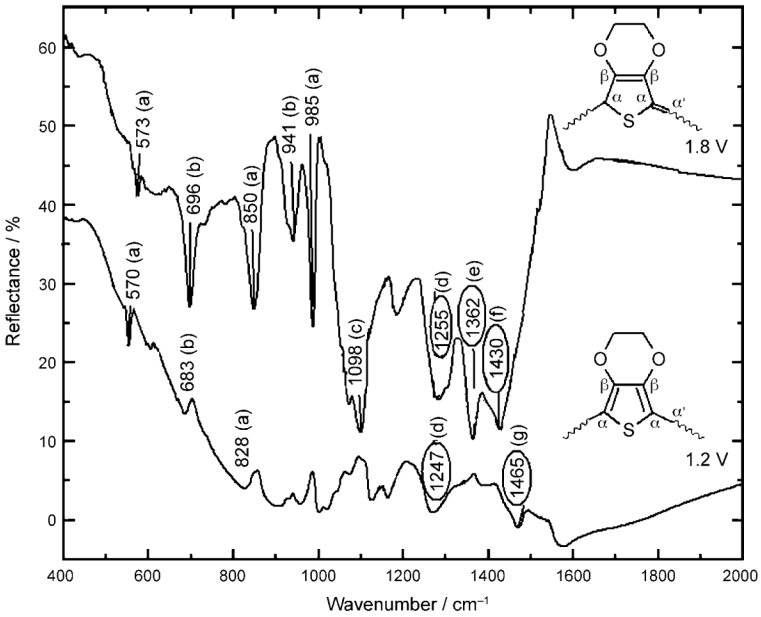

Figure 5. FTIR spectra of a) PEDOT-Vio (1.8) and b) PEDOT-Vio (1.2) films in the 400–2000 cm^{-1} wavenumber region in reflectance mode; a) oxyethylene ring deformation, b) symmetric [C–S–C] deformation, c) [C–O–C] deformation, d) [C_α–$C_{\alpha'}$] inter-ring symmetric stretching, e) [C_β–C_β] symmetric stretching, f) [C_α–C_β(-O)] symmetric stretching, and g) [C_α=C_β(-H)] symmetric stretching vibrations.

indicating the electrochromic activity of the viologen dopant. On raising the negative potential from −0.6 to −1.5 V in steps of 0.1 V, the bipolaronic peak is lost and the peak due to π-π* transition at 573 nm gains intensity (Figure 7b). With increasing magnitude of the reduction potential, even the viologen dopant's peak at 301 nm experiences an intensity increase (inset of Figure 7b). This peak at λ_{max} increases as the neutral viologen reduces to form the radical cation. As PEDOT is reduced and darkens with increase in negative potential, the cathodically coloring viologen dopant also gets reduced and complementarily enhances the level of purple coloration of the film. The redox chemistry in the electrolyte for the films is expressed in Equation (2) where $(N^+)(SO_3)^-$ is the abbreviation for *N*,*N*′-bis(3-sulfonatopropyl)-4-4′-bipyridinium.

$$(PEDOT)^{(x+y_1)^+} : (N^+)_{(x-y_2)}(SO_3^-)_x : (ClO_4)_{y_1}^- \underset{\text{reduction}}{\overset{\text{oxidation}}{\rightleftharpoons}} (PEDOT)^{(x)^+} : (N^+)_x(SO_3^-)_x + y_1(ClO_4^-)_{y_1} + y_2e^- \quad (2)$$

The redox chemistry of the neat viologen along with the detailed description of oxidation and reduction phenomena in the PEDOT-Vio (1.8) and PEDOT-Vio (1.2) films can be found in the Supporting Information (Figure S2).

Under an applied $E = -1.5$ V (this corresponds to the potential for maximum reduction), in PEDOT-Vio (1.2) (Figure 7a), the

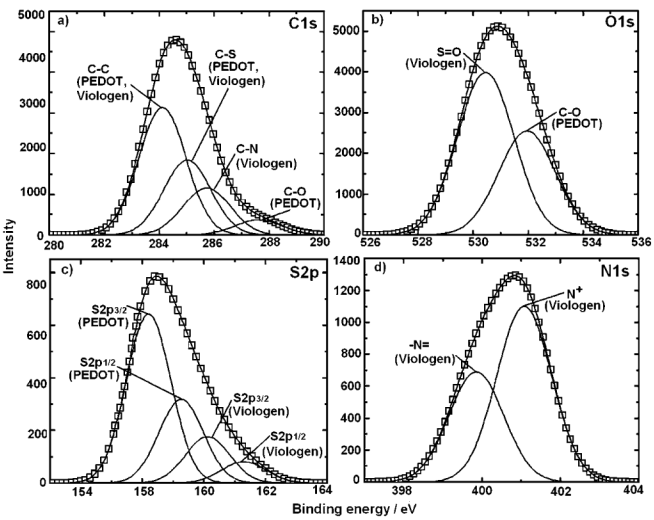

Figure 6. Core level spectra of functionalized PEDOT-Vio (1.8) film with solid lines signifying the deconvoluted contributions of a) C(1s), b) O(1s), c) S(2p), and d) N(1s).

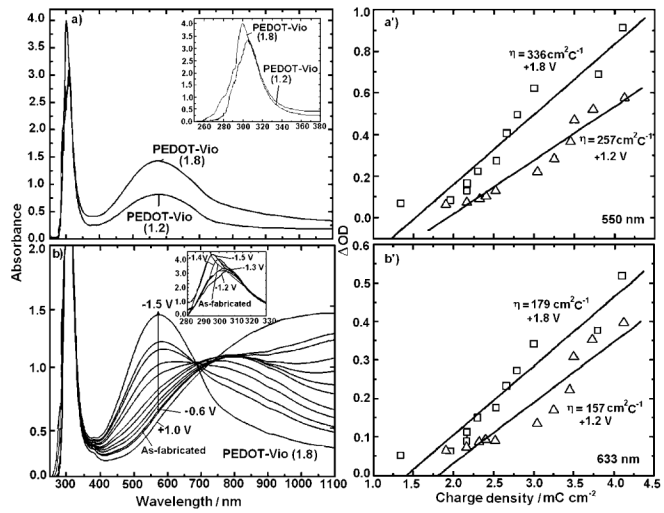

Figure 7. a) Absorbance versus wavelength plots of PEDOT-Vio (1.8) and PEDOT-Vio (1.2) films under a reduction potential of −1.5 V, inset of (a) shows a magnified view of the viologen absorption; b) absorption spectra of PEDOT-Vio (1.8) film recorded under different reduction potentials varied from −0.6–−2.0 V under steps of 0.1 V and under an oxidation potential of +1.0 V. Optical density change (ΔOD) as a function of charge density at a′) $\lambda = 550$ and b′) $\lambda = 633$ nm for the PEDOT-Vio (1.8) (□) and PEDOT-Vio (1.2) (△) films.

Electro-optical studies

The impact of electrochromic zwitterionic viologen dopant on the optical properties was examined by studying the spectroelectrochemistry of the film in $LiClO_4$-PC (1 M) under different cathodic potentials varied from −0.6 to −1.5 V in steps of 0.1 V (Figure 7a and b). In PEDOT-Vio (1.8) at +1.0 V (Figure 7b), apart from the broad oxidation peak in the 800–900 nm region ascribed to the formation of bipolarons, a sharp strong peak at wavelengths below 350 nm also appeared, indi-

characteristic viologen charge transfer peak shows a red shift to 307 nm and has a lower intensity as compared to the response of PEDOT-Vio (1.8) ($\lambda_{max}=301$ nm) film. The intensity of π-π^* transition peak (Figure 7a) corresponding to PEDOT-Vio (1.2) film is lower than that of the PEDOT-Vio (1.8) film for the same area and thickness, which clearly indicates that in PEDOT-Vio (1.8) film, a larger optical density change can be realized for the same value of applied potential.

The coloration efficiencies (CE; η) of the films is defined as the change in optical density (ΔOD) for the charge (q) consumed per unit electrode area (A) [Equation (3)].[36]

$$\text{CE}\ (\eta) = \Delta\text{OD}(\lambda)/q/A = \log\ (T_b/T_c)/q/A \qquad (3)$$

Figure 7a′ and b′ show the ΔOD at two different wavelengths of 550 and 633 nm as a function of charge density. The reference state was set at +1.0 V (oxidized state) with charge densities of 1.2 and 1.8 mC cm^{-2} for PEDOT-Vio (1.8) and PEDOT-Vio (1.2) films, respectively. As can be gauged from Figure 7a′ and b′, a lower charge density suffices to impart a higher coloration efficiency to the PEDOT-Vio (1.8) film as compared to the PEDOT-Vio (1.2) film. At 550 nm, the PEDOT-Vio (1.8) film exhibits a coloration efficiency of 336 cm^{2}C^{-1} while PEDOT-Vio (1.2) film has a coloration efficiency of 257 cm^{2}C^{-1}. In both cases, the large coloration efficiency of PEDOT reflects the contribution of the viologen dopant to the electrochromic contrast. The values of coloration efficiency are not only greater than the reported values of 180 cm^{2}C^{-1} ($\lambda=585$ nm) of pristine PEDOT but also than that of some of the derivatives such as poly(propylenedioxythiophene) (PProDOT) ($\eta=285$ cm^{2}C^{-1}, $\lambda=578$ nm) and comparable to PProDOT-Me$_2$ ($\eta=375$ cm^{2}C^{-1}, $\lambda=585$ nm).[37] However, at 633 nm, coloration efficiencies are lower: 179 cm^{2}C^{-1} in PEDOT-Vio (1.8) and 157 cm^{2}C^{-1} in PEDOT-Vio (1.2) films but a large differential continues to persist between the η_{633} values.

Flexible devices of PEDOT-Vio (1.8), PEDOT-Vio (1.2 V), and PB films

The practical utility of the PEDOT-Vio (1.8) and PEDOT-Vio (1.2) films was established by fabricating flexible PEDOT-IL gel-PB devices. Photographs of the PEDOT-Vio (1.8)-based device in dark and transparent states are shown in Figure 8. The transmittance of the electrolyte film was recorded independently (see the Supporting Information, Figure S3). The electrolyte showed a transmittance greater than 85% in most of the visible region, indicating its suitability for electrochromic windows. Ionic conductivity of the electrolytic solution prior to gelation, recorded on a dc conductivity meter, was found to be 2.8×10^{-3} S cm^{-1} at 25 °C; upon gelation, it was measured by ac impedance analysis by sandwiching the electrolyte between the two SnO_2:F electrodes. The value reduced marginally to 1.2×10^{-3} S cm^{-1}, which is acceptable for device application.

The transmittance of the devices in the 300–1100 nm wavelength range was measured under different potentials applied to the PEDOT-Vio (1.8) and PEDOT-Vio (1.2) films: $\pm$0.5, $\pm$1.0, and $\pm$1.5 V, in colored and bleached states (Figure 9). The

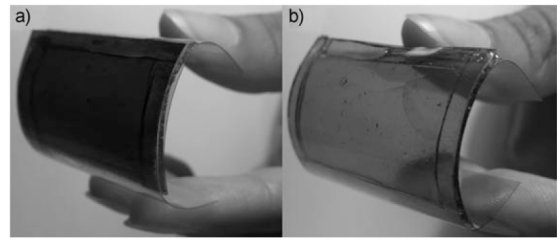

Figure 8. Digital photographs of the flexible PEDOT-Vio (1.8)-IL gel-PB device in the a) colored (E = −1.5 V) and b) bleached (E = +1.5 V) states.

transmittance minima in Figure 9a and b for both the devices (ca. 750 nm) at −1.5 V arises due to the oxidized PEDOT. This λ_{min} shows a red shift as the negative potential is decreased due to a progressive reduction in the dedoping level. However, for the PEDOT-Vio (1.2)-IL gel-PB device (Figure 9b), the λ_{min} at −1.5 V has a unusually higher intensity in comparison to its amplitude at −0.5 and −1.0 V, which suggests that film degradation is activated at high reduction potentials. The maximum transmission modulation (ΔT) of 20% at 568 nm in the PEDOT-Vio (1.8)-IL gel-PB device is observed under $\pm$1.5 V, whereas for the PEDOT-Vio (1.2)- IL gel-PB device, it is lower (ca. 12% at 501 nm). Here, ΔT varies from 17 to 20% in the visible region and then gradually drops to 8% at 1100 nm for the PEDOT-Vio (1.8)-IL gel-PB device. A similar trend, albeit lower modulation values, is observed at other potentials. In PEDOT-Vio (1.2)- IL gel-PB device, the value drops to zero ($\lambda=1100$ nm) at $\pm$1.5 V. These values are slightly lower than the ΔT of 27% of 2,5-bis-(trimethylsilyl)-PEDOT and poly(3,6-bis(3,4-ethylenedioxythiophene)-*N*-methylcarbazole) devices and 32% of PEDOT and poly(3,6-bis(3,4-ethylenedioxythiophene)-*N*-eicosylcarbazole) devices.[4]

The wavelength dependence of the coloration efficiencies of two devices is shown in Figure 9a′ and b′. For the PEDOT-Vio (1.8)-IL gel-PB device, the coloration efficiency maximum shows a monotonic increase with increase in the applied potential from $\pm$0.5 to $\pm$1.5 V (Figure 9a′). A similar trend is observed for the PEDOT-Vio (1.2)-IL gel-PB device. A sharp λ_{max} in the UV region is also observed in the spectra owing to the oxidation–reduction of the viologen dopant in PEDOT. In the PEDOT-Vio (1.8)-IL gel-PB device, this maximum is observed under all dc conditions at 382 nm, whereas in the PEDOT-Vio (1.2)-IL gel-PB device, it is present only under $\pm$1.5 V. The maximum coloration efficiency for the PEDOT-Vio (1.8)-IL gel-PB device is 187 cm^{2}C^{-1} at 693 nm whereas the PEDOT-Vio (1.2)-IL gel-PB device registered a $\eta_{max}=117$ cm^{2}C^{-1} at 528 nm. The complex capacitance response of the devices measured at different dc oxidation and reduction potentials are shown in the Supporting Information (Figure S4). From the complex capacitance curves of the two devices measured under different dc oxidation and reduction potentials, larger magnitudes of $C_{\omega\to0}$ were observed for the PEDOT-Vio (1.8)- IL gel-PB device during coloring and bleaching, which indicates a larger internal surface area or a greater number of redox active sites in the PEDOT-Vio (1.8) film that are in contact with the electrolyte anions.

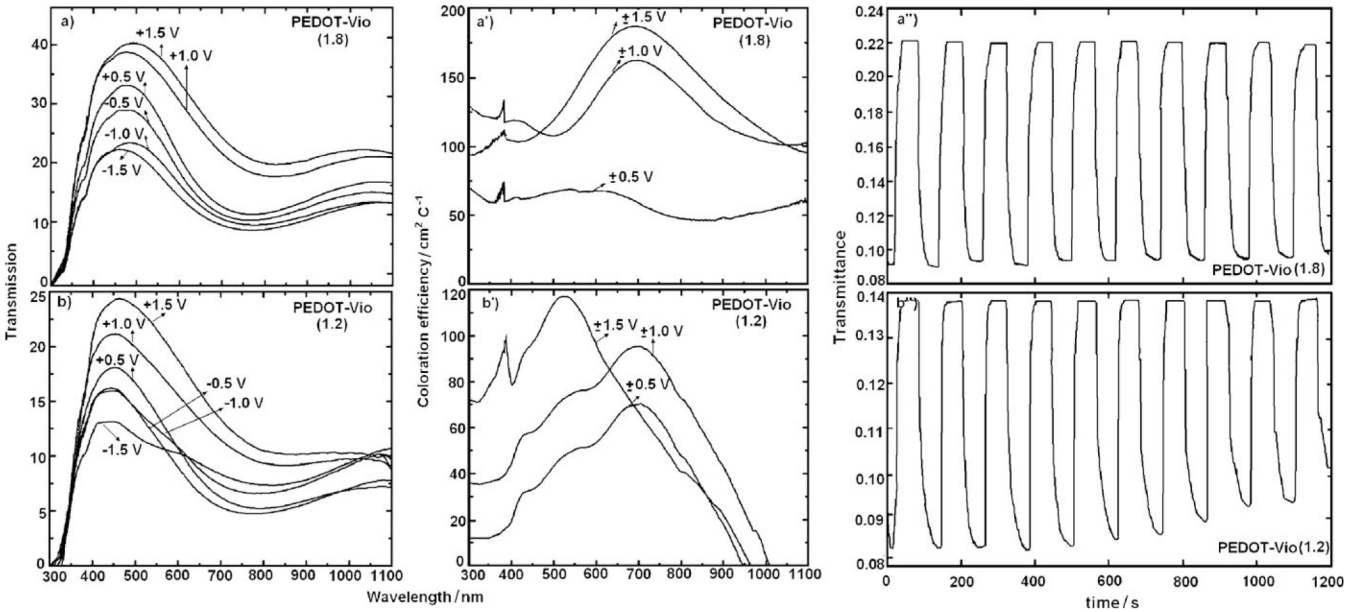

Figure 9. Transmission spectra of a) PEDOT (1.8)-IL gel-PB device and b) PEDOT-Vio (1.2)- IL gel-PB device and coloration efficiency plots as a function of wavelength of a′) PEDOT-Vio (1.8)- IL gel-PB and b′) PEDOT-Vio (1.2)- IL gel-PB devices calculated from changes in transmission, under potentials of ± 1.5, ± 1.0, and ± 0.5 V. Variation of transmittance as a function of time at $\lambda = 632.8$ nm for a′′) PEDOT-Vio (1.8)- IL gel-PB and b′′) PEDOT-Vio (1.2)-IL gel-PB devices under a square wave dc potential of ± 1.5 V at a frequency of 0.009 Hz.

Optical switching studies of the devices performed at a monochromatic wavelength of 632.8 nm, by applying alternate square wave potentials of +1.5 and −1.5 V, are shown in Figure 9a′′ and b′′. At an optimized frequency of 0.009 Hz, the transmission modulation of PEDOT-Vio (1.2)-IL gel-PB device is smaller as compared to PEDOT-Vio (1.8)-IL gel-PB device owing to a higher charge storage capacity and facile ion transfer. The modulation of PEDOT-Vio (1.2)-IL gel-PB device is only 66% of the total modulation shown by the PEDOT-Vio (1.8)-IL gel-PB device. Response times to attain colored and bleached states were determined from the time taken by the device to undergo a decrease in its transmittance from 90% to 10% and an increase from 10% to 90%, respectively, of its full response. The PEDOT-Vio (1.2)-IL gel-PB device requires 30 s to color and 8 s to bleach whereas PEDOT-Vio (1.8)-IL gel-PB device shows a faster kinetics; it colors in 15 s and bleaches in 6 s, which indicates an easy diffusion of the anions due to a more porous morphology of the PEDOT-Vio (1.8) film. Furthermore, the amplitude of the transmission modulation also decreases for PEDOT-Vio (1.2)-IL gel-PB device upon repetitive cycling, which suggests poor endurance to cycling. The switching times are larger than previously reported values for PEDOT based films[20,38] and devices.[39,40] The high sheet resistance of the underlying conducting substrate ($< 350\ \Omega\,sq^{-1}$), the interfacial resistance of the PEDOT/electrolyte, or PB/electrolyte interface are possible reasons for slow kinetics.

Conclusions

A simple route for synthesizing a dual electrochrome of PEDOT-doped by a viologen by using a zwitterionic viologen salt *N*,*N*′-bis(3-sulfonatopropyl)-4-4′-bipyridinium as a source of charge compensating anions during electropolymerization of PEDOT, has been demonstrated. The resulting thin-film nanostructures of viologen-doped PEDOT comprised of 1) a regular particulate structure and (2) dendritic shapes superimposed on a granular phase, when grown at oxidation potentials of +1.2 and +1.8 V, respectively. Distinct signals due to nitrogen in the core level XPS spectrum and the characteristic absorptions of the bipyridinium moiety in the electro-optical response of the film, affirmed that the viologen is not an adventitious entity but is an inherent part of the polymer chain. The dendritic morphology achieved in the PEDOT-Vio (1.8) film, imparted a higher coloration efficiency and improved electrochemical activity as compared to the PEDOT-Vio (1.2) film. Redox switching between pale to deep purple and vice-versa, achieved in a flexible electrochromic device with the PEDOT-Vio (1.8) film and an IL gel polymer electrolyte, showed fast response times, high diffusional capacitance, and a coloring efficiency of 187 $cm^2\ C^{-1}$ in the visible region; these performance attributes unambiguously justify the applicability of PEDOT-Vio (1.8) films to smart windows.

Experimental

Materials

3,4-ethylenedioxythiophene (EDOT), 4-4′-bipyridine, 1,3-propane sultone, and polyvinyl alcohol (MW: 86 000–124 000, dried for 24 h at 80 °C prior to use) were obtained from Aldrich and ferric chloride was obtained from Qualigens. Ionic liquid: 1-butyl-1-methylpyrrolidiniumtrifluoromethanesulfonate,
Tween 20 (polyoxyethylene sorbitan monolaurate), potassium ferricyanide, and reagents dimethyl sulfoxide and ethanol were

obtained from Merck and used as received. Deionized water (resistivity ca. 18.2 MΩcm) was obtained through Milli-Q system. Inorganic transparent electrodes of SnO_2:F coated glass (Pilkington, sheet resistance: 14 Ωsq^{-}) were cleaned in a soap solution, 30% HCl solution, double distilled water, and acetone prior to use. For devices, polyethylene terephthalate (PET)-based transparent substrates coated with a conductive layer of PEDOT-poly(styrenesulfonate) (PEDOT:PSS) (Orgacon, sheet resistance $< 350\ \Omega sq^{-1}$, base thickness of about 125 μm) were washed with deionized water and dried in air prior to use.

Synthesis of dopant *N*,*N*′-bis(3-sulfonatopropyl)-4-4′-bipyridinium

N,*N*′-bis(3-sulfonatopropyl)-4-4′-bipyridinium was prepared by refluxing 4,4′-bipyridine (1.5 g) with 1,3-propane sultone (8.0 g) for 15 min at 120 °C without solvent under nitrogen. To the resulting semi-solid mixture, dimethyl sulfoxide (60 mL) was injected and heated at 120 °C while being stirred continuously for 3 h. After cooling, the white precipitate of the viologen *N*,*N*′-bis(3-sulfonatopropyl)-4-4′-bipyridinium was filtered and washed several times with methanol, dried over Whatman 42 filter papers, and stored at temperatures less than 10 °C (yield ca. 71%). ^{1}H NMR (300 MHz, D_2O): δ (ppm) = 9.1 (d, J = 1.0 Hz, 4H), 8.5 (d, J = 1.02 Hz, 4H), 4.8 (t, J = 1.0 Hz, 4H), 2.9 (t, J = 1.02 Hz, 4H), 2.5 (m, 4H).

Deposition of PEDOT and PB films

PEDOT films were electropolymerized from an aqueous formulation containing EDOT (0.1 M), Tween 20 (0.1 M) as surfactant and *N*,*N*′-bis(3-sulfonatopropyl)-4-4′-bipyridinium (0.1 M), potentiostatically at two different potentials of +1.2 and +1.8 V for 120 s at room temperature. Optically transparent SnO_2:F-coated glass and PEDOT:PSS coated PET substrates were used as working electrodes, Ag/AgCl/KCl as a reference and a platinum sheet as a counter electrode. The purple films were first rinsed in deionized water and dried in air prior to use. Prussian blue (PB) films were grown galvanostatically on conductive PEDOT:PSS-coated PET substrates in a two electrode configuration with a platinum sheet as a counter electrode from a solution of ferric chloride (10 mM) and potassium ferricyanide (10 mM) in HCl (0.01 N in deionized water) for 8 min under a constant current of 10 $\mu A\,cm^{-2}$ applied by a Keithley 2400 current source. The films were rinsed in deionized water and dried in air.

Electrolyte synthesis and fabrication of flexible devices

To synthesize polymer electrolyte, 6 wt% of polyvinyl alcohol was dissolved in a solution of 1-butyl-1-methylpyrrolidiniumtrifluoromethanesulfonate (0.2 M) in dimethyl sulfoxide at 70 °C with rigorous stirring for 8 h. The resulting transparent viscous solution was poured into a prefabricated cavity made on the PB film created using a spacer (transparent acrylic tape, 1 mm thick and 5 mm wide) placed along the periphery of the film. This assembly was left undisturbed at room temperature for 48 h for gelation and self-supporting film formation. Subsequent to electrolyte film formation, PEDOT film deposited over PEDOT:PSS-coated PET substrate was placed over the PB film such that the electrolyte film lied in between. The device components were held together firmly with binder clips to avoid bubble formation and to allow the acrylic tape to adhere with the two films; the clips were removed only after 24 h. Finally, a cyanoacrylate adhesive was used for sealing the device.

Characterization techniques

FTIR spectra for the PEDOT films were recorded in the reflection mode with a specular reflectance accessory on a Perkin–Elmer Spectrum BX spectrophotometer at 28 °C; the angle of incidence was fixed at 35°. The surface morphological features of the films were investigated using a SEM (LEO 440) after sputtering a thin layer of gold on the film surface. TEM was carried out by transferring the sample onto a carbon-coated copper grid on a HRTEM Tecnai G^2 F30 STWIN with a FEG source at 300 kV. XPS spectra were recorded, for the as-synthesized PEDOT films, on a Perkin–Elmer 1257 model operating at a base pressure of 2.4x 10^{-8} Torr at 300 K with a non-monochromatized AlK_α line at 1486.6 eV, an analyzer pass energy of 60 eV, and a hemispherical sector analyzer capable of 25 meV resolution. The overall instrumental resolution was about 0.3 eV. The core level spectra were deconvoluted by using a nonlinear iterative least squares Gaussian fitting procedure. For all fitting doublets, the FWHMs were fixed accordingly. Corrections due to the charging effects were taken care of by using C(1s) as an internal reference and the Fermi edge of a gold sample. Cyclic voltammetry (CV) for the films was performed in a classical three-electrode electrochemical cell, wherein the PEDOT film acted as the working electrode, an Ag/Ag^+ was employed as the reference electrode, and a Pt rod was used as the counter electrode in a liquid electrolyte (1 M $LiClO_4$-propylene carbonate (PC)). The CV response of the viologen was recorded for a 0.2 M aqueous solution with Ag/Ag^+ as the reference electrode and two Pt rods were used as the working and counter electrodes. Absorbance spectra for colored and bleached PEDOT films were recorded ex situ in the 300–1100 nm wavelength range on a Perkin–Elmer Lambda 25 spectrophotometer as films were found to exhibit an open-circuit memory of about 60–120 s, in a controlled temperature and humidity chamber (approximately 22–25 °C, relative humidity ca. 48–52%). The films were colored under different reduction potentials varying from −0.6 to −2.0 V for a fixed duration of 60 s in a liquid electrolyte (1 M $LiClO_4$-PC) at each potential. Electrochemical impedance spectroscopy measurements were performed on the PEDOT-IL gel-PB device under different dc bias potentials superimposed over an ac amplitude of 10 mV with PEDOT as the working electrode. Switching time characteristics for the device between colored and bleached states were recorded with an automated setup consisting of a He–Ne laser (λ = 632.8 nm), a Si photodetector, and a custom made microprocessor controlled versatile unit. The device was illuminated with the laser beam and a photodiode was used to

sense the light intensity transmitted through the device. The transmittance versus time transients were recorded at a frequency of 0.009 Hz, when a square wave potential of ± 1.5 V was applied to the device. All electrochemical deposition and measurements were performed on a Gamry Reference 600 potentiostat/galvanostst/ZRA coupled with PHE 200/EIS 300 softwares, unless specified otherwise.

Acknowledgements

The authors thank NPL for financial support. S.B. acknowledges the University Grants Commission (UGC) for a senior research fellowship. We thank Dr. S. T. Lakshmikumar (National Physical laboratory) for his guidance and encouragement. We also thank Orgacon for free samples of PEDOT:PSS substrates.

Keywords: doping · electrochemistry · electrochromism · redox chemistry · zwitterions

[1] P. M. S. Monk, R. J. Mortimer, D. R. Rosseinsky, *Electrochromism and Electrochromic Devices*, 1 st Ed., Cambridge Univ. Press, UK, **2007**.
[2] R. J. Mortimer, *Chem. Soc. Rev.* **1997**, *26*, 147 – 156.
[3] A. M. Nardes, M. Kemerink, R. A. J. Janssen, J. A. M. Bastiaansen, N. M. M. Kiggen, B. M. W. Langeveld, A. J. J. M. Van Breemen, M. M. de Kok, *Adv. Mater.* **2007**, *19*, 1196 – 1200.
[4] S. A. Sapp, G. A. Sotzing, J. R. Reynolds, *Chem. Mater.* **1998**, *10*, 2101 – 2108.
[5] C. Kvarnström, H. Neugebauer, S. Blomquist, H. J. Ahonen, J. Kankare, A. Ivaska, *Electrochim. Acta* **1999**, *44*, 2739 – 2750.
[6] K. Krishnamoorthy, M. Kanungo, A. Q. Contractor, A. Kumar, *Synth. Met.* **2001**, *124*, 471 – 475.
[7] I. F. Perepichka, E. Leviallain, M. Salle, J. Roncali, *Chem. Mater.* **2002**, *14*, 449 – 457.
[8] J. L. Segura, R. Gomez, R. Blanco, E. Reinold, P. Bauerle, *Chem. Mater.* **2006**, *18*, 2834 – 2847.
[9] C. A. Cutler, M. Bouguettaya, T-S. Kang, J. R. Reynolds, *Macromolecules* **2005**, *38*, 3068 – 3074.
[10] H. C. Ko, M. Kang, B. Moon, H. Lee, *Adv. Mater.* **2004**, *16*, 1712 – 1716.
[11] M. Besbes, G. Trippe, E. Leviallain, M. Mazari, F. Le Derf, I. F. Perepichka, A. Devdour, A. Gorgues, M. Salle, J. Roncali, *Adv. Mater.* **2001**, *13*, 1249 – 1252.
[12] J. Stepp, J. B. Schlenoff, *J. Electrochem. Soc.* **1997**, *144*, L155L157.
[13] D. M. DeLongchamp, M. Kastantin, P. T. Hammond, *Chem. Mater.* **2003**, *15*, 1575 – 1586.
[14] E. M. Girotto, M- A. DePaoli, *Adv. Mater.* **1998**, *10*, 790 – 793.
[15] M. V. Rosenthal, T. A. Skotheim, C. A. Linkous, *Synth. Met.* **1986**, *15*, 219 – 227.
[16] C. S. Choi, H. Tachikawa, *J. Am. Chem. Soc.* **1990**, *112*, 1757 – 1768.
[17] O. Ikeda, K. Okabayashi, N. Yoshida, H. Tamura, *J. Electroanal. Chem.* **1985**, *191*, 157 – 174.
[18] H-K. Song, E. J. Lee, S. M. Oh, *Chem. Mater.* **2005**, *17*, 2232 – 2233.
[19] S. Cho, S. B. Lee, *Acc. Chem. Res.* **2008**, *41*, 699 – 707.
[20] S. Cho, D. H. Choi, S-H. Kim, S. B. Lee, *Chem. Mater.* **2005**, *17*, 4564 – 4566.
[21] R. Xiao, S. Cho, R. Liu, S. B. Lee, *J. Am. Chem. Soc.* **2007**, *129*, 4483 – 4489.
[22] H. Randriamahazaka, V. Noel, C. Chevrot, *J. Electroanal. Chem.* **1999**, *472*, 103 – 111.
[23] M. Deepa, S. Bhandari, R. Kant, *Electrochim. Acta* **2009**, *54*, 1292 – 1303.
[24] A. J. Bard, L. R. Faulkns, *Electrochemical Methods: Fundamentals and Applications*, 2nd Ed., Wiley, New York, **2001**.
[25] S. Bhandari, M. Deepa, S. Singh, G. Gupta, R. Kant, *Electrochim. Acta* **2008**, *53*, 3189 – 3199.
[26] M. Deepa, S. Bhandari, M. Arora, R. Kant, *Macromol. Chem. Phys.* **2008**, *209*, 137 – 149.
[27] Y. Xiao, C. M. Li, S. Yu, Q. Zhou, V.-S. Lee, S. M. Moochhala, *Talanta* **2007**, *72*, 532.
[28] K. E. Aasmundtveit, E. J. Samuelsen, L. A. A. Pettersson, O. Inganas, T. Johansson, R. Feidenhans'l, *Synth. Met.* **1999**, *101*, 561 – 564.
[29] S. Bhandari, M. Deepa, A. K. Srivastava, A. G. Joshi, R. Kant, *J. Phys. Chem. B* **2009**, *113*, 9416 – 9428.
[30] S. Garreau, G. Louarn, J. B. Buisson, G. Froyer, S. Lefrant, *Macromolecules* **1999**, *32*, 6807 – 6812.
[31] J. Ouyang, C.-W. Chu, F-C. Chen, Q. Xu, Y. Yang, *Adv. Funct. Mater.* **2005**, *15*, 203 – 208.
[32] W. W. Chiu, T. Travas-Sejdic, R. P. Coney, G. A. Bowmaker, *J. Raman Spectrosc.* **2006**, *37*, 1354 – 1361.
[33] N. Sakmeche, S. Aeiyach, J. J. Aaron, M. Jouini, J. C. Lacroix, P.-C. Lacaze, *Langmuir* **1999**, *15*, 2566 – 2574.
[34] C. Li, T. Imae, *Macromolecules* **2004**, *37*, 2411 – 2416.
[35] S. W. Ng, K. G. Neoh, Y. T. Wang, J. T. Sampanthar, E. T. Kang, K. L. Tan, *Langmuir* **2001**, *17*, 1766 – 1772.
[36] C. G. Ganqvist, in *Handbook of Inorganic Electrochromic Materials*, Elsevier Science, Amsterdam, **1995**.
[37] C. G. Gaupp, D. M. Welsh, R. D. Rauh, J. R. Reynolds, *Chem. Mater.* **2002**, *14*, 3964 – 3970.
[38] A. Kumar, D. M. Welsh, M. C. Morvant, F. Piroux, K. A. Abboud, J. R. Reynolds, *Chem. Mater.* **1998**, *10*, 896 – 902.
[39] T.-H. Lin, K.-C. Ho, *Sol. Energy Mater. Sol. Cells* **2006**, *90*, 506 – 520.
[40] M. Deepa, A. Awadhia, S. Bhandari, *Phys. Chem. Chem. Phys.* **2009**, *11*, 5674 – 5685.